



Published in final edited form as:

*J Labelled Comp Radiopharm.* 2014 February ; 57(2): 86–91. doi:10.1002/jlcr.3168.

## **<sup>18</sup>F-Fluorodeoxyglycosylamines: Maillard reaction of <sup>18</sup>F-fluorodeoxyglucose with biological amines†**

**Aparna Baranwal, Himika H. Patel, and Jogeshwar Mukherjee\***

Preclinical Imaging, Department of Radiological Sciences, University of California – Irvine, Irvine, CA 92697, USA

### **Abstract**

The Maillard reaction of sugars and amines resulting in the formation of glycosylamines and Amadori products is of biological significance, for drug delivery, role in central nervous system, and other potential applications. We have examined the interaction of <sup>18</sup>F-fluorodeoxyglucose (<sup>18</sup>F-FDG) with biological amines to study the formation of <sup>18</sup>F-fluorodeoxyglycosylamines (<sup>18</sup>F-FDGly). Respective amines *N*-allyl-2-aminomethylpyrrolidine (NAP) and 2-(4'-aminophenyl)-6-hydroxybenzothiazole (PIB precursor) were mixed with FDG to provide glycosylamines, FDGNAP and FDGBTA. Radiosynthesis using <sup>18</sup>F-FDG (2–5 mCi) was carried out to provide <sup>18</sup>F-FDGNAP and <sup>18</sup>F-FDGBTA. Binding of FDGBTA and <sup>18</sup>F-FDGBTA was evaluated in human brain sections of Alzheimer's disease (AD) patients and control subjects using autoradiography. Both FDGNAP and FDGBTA were isolated as stable products. Kinetics of <sup>18</sup>F-FDGNAP reaction indicated a significant product at 4 h (63% radiochemical yield). <sup>18</sup>F-FDGBTA was prepared in 57% yield. Preliminary studies of FDGBTA showed displacement of <sup>3</sup>H-PIB (reduced by 80%), and <sup>18</sup>F-FDGBTA indicated selective binding to A $\beta$ -amyloid plaques present in postmortem AD human brain, with a gray matter ratio of 3 between the AD patients and control subjects. We have demonstrated that <sup>18</sup>F-FDG couples with amines under mild conditions to form <sup>18</sup>F-FDGly in a manner similar to click chemistry. Although these amine derivatives are stable in vitro, stability in vivo and selective binding is under investigation.

### **Keywords**

<sup>18</sup>F-FDG; Maillard reaction; quasi-Amadori product

### **Introduction**

The Maillard reaction of sugars and amines results in the formation of glycosylamines and Amadori products.<sup>1</sup> These are of great biological significance, for drug delivery as prodrugs, role in central nervous system, and other potential applications.<sup>2,3</sup> The formation of Amadori product occurs by the reaction of the amine with the aldehyde at the 1-position of glucose to

†Presented at the Annual Meeting of the Society of Nuclear Medicine, Vancouver, Canada, June 8–12, 2013.

\*Correspondence to: Jogesh Mukherjee, B138 Medical Sciences, Department of Radiological Sciences, University of California – Irvine, Irvine, CA 92697-5000, USA. j.mukherjee@uci.edu.

#### **Conflict of Interest**

The authors did not report any conflict of interest.

form a Schiff base **3** (Figure 1), followed by dehydration and rearrangement of the hydroxyl at the 2-position to form a ketone **5** (Figure 1).<sup>4,5</sup> It has been shown that glucose reacts with serotonin to undergo the Maillard reaction and produce an Amadori product, **6** desoxyfructoserotonin.<sup>6</sup> This Amadori product has been used to elevate brain serotonin levels in mice studies.<sup>3</sup> Maillard reaction products have been observed and assessed in aging, diabetes, and Alzheimer's disease (AD) pathologies.<sup>7,8</sup>

Glycosylamines are significant in various aspects of human physiology. Involved in the characterization of glycoprotein and glycopeptides, glycosylamines have become an area of interest because of their involvement in metabolic pathways. An Amadori product obtained from the Maillard reaction is fructoselysine **7** (Figure 1) that is present in tissue proteins.<sup>7</sup>

2-<sup>18</sup>F-Fluorodeoxyglucose **8** ([<sup>18</sup>F]FDG; Figure 2), a 2-deoxy analog of glucose is used clinically in various studies for evaluating alterations in glucose metabolic rates using positron emission tomography.<sup>9,10</sup> [<sup>18</sup>F] FDG is phosphorylated by hexokinase and is trapped in the cell in the form of [<sup>18</sup>F]FDG-6-phosphate because of the absence of the hydroxyl group at the 2' position of glucose. Because [<sup>18</sup>F]FDG contains the aldehyde group, but lacks the hydroxyl group at the 2'-position, it is potentially capable of undergoing the Maillard reaction with amines to form the Schiff base **10** ([<sup>18</sup>F]FDGly, a quasi-Amadori product; Figure 2) without progressing to the classical Amadori product as shown in Figure 1.<sup>4</sup>

Our goal here was to examine if fluorodeoxyglucose (FDG) reacts with simple amines to form the Maillard reaction products. In this paper, we have investigated the following: (1) the formation of fluorodeoxyglycosylamines (FDGly) as shown in Figure 2 using the model amine *N*-allyl-2-aminomethylpyrrolidine (NAP) to generate fluorodeoxyglycosyl-*N*-allyl-2-aminomethylpyrrolidine (FDGNAP), **11** (Figure 2). This methodology was then extended to biological amines of interest that may interact with A $\beta$ -amyloid plaque, 2-(4'-aminophenyl)-6-hydroxybenzothiazole (BTA) to form fluorodeoxyglycosyl-2-(4'-aminophenyl)-6-hydroxybenzothiazole (FDGBTA), **12** (Figure 2); (2) radiosynthesis of <sup>18</sup>F-FDGNAP and <sup>18</sup>F-FDGBTA; and (3) biological evaluation of FDGBTA and <sup>18</sup>F-FDGBTA.

## Materials and methods

### General methods

All chemicals and solvents were of analytical or HPLC grade from (Aldrich Chemical Co., Milwaukee, WI USA) and (Fisher Scientific, Inc., Pittsburgh, PA USA). 2-(4'-Aminophenyl)-6-hydroxybenzothiazole (also referred as 6-OH-BTA-0) was purchased from ABX Chemicals, Radeberg, Germany. Electrospray mass spectra were obtained on a Model 7250 mass spectrometer (Micromass LCT, Waters, Milford, MA USA). Proton NMR spectra were recorded on a (Bruker Biospin Corporation, Billerica, MA USA) OMEGA 500 MHz spectrometer. Analytical thin layer chromatography (TLC) was carried out on silica coated plates (Baker-Flex, Phillipsburg, NJ, USA). Chromatographic separations were carried out on preparative TLC (silica gel GF 20  $\times$  20 cm, 2000  $\mu$ m thick; Alltech Assoc. Inc., Deerfield, IL, USA) or silica gel flash columns or semi-preparative reverse-phase columns using the (Gilson, Inc., Middleton, WI USA) HPLC systems. <sup>18</sup>F-FDG was obtained from

(PETNET, Culver City, CA USA) in sterile saline solution. Fluorine-18 radioactivity was counted in a Capintec dose calibrator while low level counting was carried out in a well-counter (Cobra quantum, Packard Instruments Co., Boston, MA, USA). Radioactive thin layer chromatographs were obtained by scanning in a Bioscan system 200 Imaging scanner (Bioscan, Inc., Washington, DC, USA). Human postmortem brain slices were obtained on a (Leica Microsystems Inc., Deerfield, IL USA) 1850 cryotome. Fluorine-18 autoradiographic studies were carried out by exposing tissue samples on storage phosphor screens. The apposed phosphor screens were read and analyzed by (OptiQuant, Perkinelmer. Walthman, MA USA) acquisition and analysis program of the Cyclone Storage Phosphor System (Packard Instruments Co.).

## Synthesis

**FDGNAP**—To synthesize FDGNAP, 7  $\mu\text{l}$  ( $5.50 \times 10^{-5}$  mol) of NAP and 5.0 mg ( $2.75 \times 10^{-5}$  mol) of FDG were dissolved in 0.2 ml acetate buffer (0.1 M sodium acetate-acetic acid, pH4.2) and 5  $\mu\text{l}$  aniline as a catalyst. The solution was left at room temperature for 4 h. Preparatory TLC was performed using 9:1 dichloromethane/methanol to provide FDGNAP in 31% yield. Mass Spectrometry (MS):  $m/z$  305  $[\text{M} + \text{H}]^+$ . Aniline used as a catalyst also showed small amounts (approximately 20–30%) of the FDG adduct (MS:  $m/z$  280  $[\text{M} + \text{Na}]^+$ ).

**FDGBTA**—For the synthesis of FDGBTA, 2.0 mg ( $3.29 \times 10^{-5}$  mol) of BTA and 1.5 mg ( $1.65 \times 10^{-5}$  mol) of FDG were dissolved in 0.25 ml EtOH. The solution was heated for 1 h at 99 °C. Retention time of BTA was 11.3 min while that of FDGBTA was 7.5 min (reverse-phase 10  $\mu\text{m}$  C-18 HPLC column, 10  $\times$  250 mm, 40% 0.1% triethylamine in water:60% acetonitrile, flow rate 1.5 ml/min). Preparatory TLC was performed using 9:1 dichloromethane/methanol solvent to extract FDGBTA in 58% yield. MS:  $m/z$  429  $[\text{M} + \text{Na}]^+$  (Figure 3).

## Radiosynthesis

**$^{18}\text{F}$ -FDGNAP**—To synthesize  $^{18}\text{F}$ -FDGNAP (**15**), 9  $\mu\text{l}$  aniline catalyst and 5  $\mu\text{l}$  NAP (**13**) were dissolved in 0.1 ml acetate buffer, and 0.1 ml of 1 mCi  $^{18}\text{F}$ -FDG (**8**, in 0.9% sterile saline) was added to this mixture. The reaction was monitored by radio-TLC at 0.17, 1, 2, 3, and 4 h using the Optiquant software, and the product was confirmed by coelution of reference standard.

**$^{18}\text{F}$ -FDGBTA**—For the synthesis of  $^{18}\text{F}$ -FDGBTA (**18**), 1 mg ( $4.13 \times 10^{-6}$  mol) BTA (**16**) was dissolved in 0.2 ml EtOH and 0.1 ml of 2 to 5 mCi.  $^{18}\text{F}$ -FDG (**8**, in 0.9% sterile saline) was dissolved in the solution. The solution was heated for 2 h at 99 °C. Preparatory TLC (9:1 dichloromethane/methanol) was used to isolate and purify  $^{18}\text{F}$ -FDGBTA ( $r_f = 0.3$  for  $^{18}\text{F}$ -FDGBTA). The purified  $^{18}\text{F}$ -FDGBTA (**18**) was obtained in 57% radiochemical yield with specific activities of approximately 1000 Ci/mmol (Figure 4). This was used for biological studies.

## In vitro studies

**<sup>3</sup>H-PIB binding**—Human hippocampus sections (7 μm thick) were preincubated in 10% alcohol Phosphate Buffered Saline (PBS) buffer for 10 min. The brain sections were placed in a glass chamber and incubated with <sup>3</sup>H-PIB (2 μCi/cc) in 10% alcohol PBS buffer, pH 7.4 at 37 °C for 1 h. The slices were then washed with cold 10% alcohol PBS buffer (2 × 3 min) and cold deionized water for 1 min. The brain sections were air dried, exposed overnight on a phosphor film, and then placed on the Phosphor Autoradiographic Imaging System/Cyclone Storage Phosphor System (Packard Instruments Co.). Regions of interest (ROIs) were drawn on the slices, and the extent of binding of <sup>3</sup>H-PIB was measured with DLU/mm<sup>2</sup> using the OptiQuant acquisition and analysis program (Packard Instruments Co.).

**<sup>11</sup>C-PIB binding**—Human hippocampus sections (7 μm thick) were preincubated (40% EtOH:60% deionized water) for 10 min. The brain sections were placed in a glass chamber and incubated with <sup>11</sup>C-PIB (20 μCi/cc) in 40% EtOH:60% deionized water at 37 °C for 1 h. The slices were then washed with cold millipore water, 70%–90% EtOH, for 2, 1, 1, 1, and 1 min. The brain sections were air dried, exposed overnight on a phosphor film, and then placed on the Phosphor Autoradiographic Imaging System/Cyclone Storage Phosphor System (Packard Instruments Co.). ROIs were drawn on the slices, and the extent of binding of <sup>11</sup>C-PIB was measured with DLU/mm<sup>2</sup> using the OptiQuant acquisition and analysis program (Packard Instruments Co.).

**<sup>18</sup>F-FDGBTA binding**—Human hippocampus sections (7 μm thick) were preincubated in 10% alcohol PBS buffer for 10 min. The brain sections were placed in a glass chamber and incubated with <sup>18</sup>F-FDGBTA (2 μCi/cc) in 10% alcohol PBS buffer, pH 7.4 at 37 °C for 1 h. The slices were then washed with cold 10% alcohol PBS buffer (2 × 3 min) and cold deionized water for 1 min. The brain sections were air dried, exposed overnight on a phosphor film, and then placed on the Phosphor Autoradiographic Imaging System/Cyclone Storage Phosphor System (Packard Instruments Co.). ROIs were drawn on the slices, and the extent of binding of <sup>18</sup>F-FDGBTA was measured with DLU/mm<sup>2</sup> using the OptiQuant acquisition and analysis program (Packard Instruments Co.).

## Results and discussion

Fluoro-2-deoxyglucose reacted with both the primary aliphatic amine (NAP) and the substituted aniline derivative (BTA) to provide stable products, **11** and **12** (Figure 2). A classical Amadori product, similar to that found with glucose **5** (Figure 1), is not expected because of the fluorine at the 2-position in FDG. Structures **11** and **12** are Schiff bases and may be considered as quasi-Amadori products resulting from the Maillard reaction as shown in Figure 1. The fluorine present at the 2-position traps the Schiff base as a quasi-Amadori product. Reactions were carried out under aqueous and nonaqueous conditions with little effect on yields. Addition of aniline as a catalyst increased the yields as reported previously.<sup>11</sup>

Based on our findings with unlabeled FDG, an <sup>18</sup>F-FDGly quasi-Amadori product was expected from the reaction of <sup>18</sup>F-FDG with NAP and BTA. The reaction kinetics of <sup>18</sup>F-FDG with NAP at room temperature was monitored by radio-TLC at 0.17, 1, 2, 3, and 4 h

(Figure 3C and D). Over time, the  $^{18}\text{F}$ -FDGNAP product increased and the  $^{18}\text{F}$ -FDG decreased (Figure 3B). The amount of  $^{18}\text{F}$ -FDG aniline was consistently around 25–30% in solution and served as an intermediate product for the formation of  $^{18}\text{F}$ -FDGNAP.  $^{18}\text{F}$ -FDGNAP increased over time from 21% to 63% while  $^{18}\text{F}$ -FDG decreased to 10% in 4 h (Figure 3B).

The reaction of BTA with  $^{18}\text{F}$ -FDG was carried out in ethanol without the catalyst, aniline, and thus required heating. The radioactive product  $^{18}\text{F}$ -FDG BTA was purified by radio-TLC in 57% yield, and few significant side products were observed (Figure 4B).

The synthesis and radiosynthesis of FDGly occurred at room temperature by the addition of the substituted amines to FDG and may thus be akin to click chemistry.<sup>12</sup> Thus, this synthetic approach may be considered similar to click chemistry using FDG. This method may be applied generally to various amines using the simple reaction conditions described here, similar to click chemistry approaches with other substrates.<sup>13</sup> It may therefore be used for rapid radiosynthesis using  $^{18}\text{F}$ -FDG as exemplified in the preparation of  $^{18}\text{F}$ -FDGNAP and  $^{18}\text{F}$ -FDGBTA.

Because FDGBTA is an analog of PIB, which is known to bind to human  $A\beta$ -amyloid plaques, we tested the competition of both PIB and FDGBTA with postmortem human brain  $A\beta$ -amyloid sites labeled with  $^3\text{H}$ -PIB (Figure 5A). Preliminary studies indicated that at 10  $\mu\text{M}$  concentration,  $^3\text{H}$ -PIB was displaced from the  $A\beta$ -plaque binding sites by FDGBTA and PIB, and the reduction in the gray matter areas was >80% (Figure 5C). A more detailed dose–response study is planned in order to obtain the binding affinity of FDGBTA for these sites.

Radiolabeled  $^{18}\text{F}$ -FDGBTA (Figure 6D) was evaluated and compared with  $^{11}\text{C}$ -PIB (Figure 6A) for binding to postmortem human brain  $A\beta$ -amyloid sites. As expected  $^{11}\text{C}$ -PIB exhibited significant binding to AD brain gray matter as shown previously (Figure 6B), whereas binding of  $^{18}\text{F}$ -FDGBTA was found to be nonuniform but exhibited regions of high binding (Figure 6E).<sup>14</sup> Ratio of AD brain versus control subjects was 6 for  $^{11}\text{C}$ -PIB, while that for  $^{18}\text{F}$ -FDGBTA was 3. In contrast,  $^{18}\text{F}$ -FDG did not exhibit any binding to the gray matter areas of AD subjects. These findings suggest that  $^{18}\text{F}$ -FDGBTA is stable in vitro and exhibits biological properties similar to  $^{11}\text{C}$ -PIB with lower ratios, suggesting that either the affinity of FDGBTA may be lower than PIB or there may be additional sites of binding due to a significant difference in the size of the substituent ( $^{11}\text{C}$ -methyl in PIB versus  $^{18}\text{F}$ -FDG in FDGBTA).

Our preliminary studies suggest that  $^{18}\text{F}$ -FDGly are stable in vitro and exhibit biological properties. Presence of glucose-derived Amadori products have been reported in vivo and their use suggested as prodrugs (e.g., for the timed-release of serotonin).<sup>15</sup> However, there have been no in vivo studies on the Maillard reactions of deoxyglucose or FDG with various biological amines (proteins, lipids, or small molecules). Therefore, in vivo relevance of the formation of  $^{18}\text{F}$ -FDGly during  $^{18}\text{F}$ -FDG studies has yet to be determined.

## Conclusions

Fluorodeoxyglucose couples with amines under mild conditions to form FDGly, which are stable, isolated quasi-Amadori products. We have demonstrated that  $^{18}\text{F}$ -FDG couples with amines under appropriate conditions to form  $^{18}\text{F}$ -FDGly. Although these amine derivatives are stable in vitro and exhibit biological properties, stability in vivo is under investigation. Additionally, reductive amination to produce reduced FDGly is underway in order to enhance in vivo stability.

## Acknowledgments

Research support was provided by NIH AG029479 and DK092917. We like to thank Christopher Liang for technical assistance. We would like to thank Mr. Said Shokair at the Undergraduate Research Opportunities Program (UROP) of the University of California-Irvine for summer support (AB and HHP) through the ID-SURE program.

## References

1. Evans S. The Maillard reaction turns 100. *Chem Engr News*. 2012; 90:58–60.
2. Manini P, d'Ischia M, Prota G. An unusual decarboxylative Maillard reaction between L-DOPA and D-glucose under biomimetic conditions: factors governing competition with Pictet-Spengler condensation. *J Org Chem*. 2001; 66:5048–5053. [PubMed: 11463255]
3. Szabados L, Mester M, Mester L, Bhargava KP, Parvez S, Parvez H. New method to increase the serotonin level in brain by carotid injection of desoxyfructo-serotonin in mice. *Biochem Pharm*. 1982; 31:2121–2123. [PubMed: 7115431]
4. Thornalley PJ, Langborg A, Minhas HS. Formation of glyoxal, methylglyoxal and 3-deoxyglucosone in the glycation of proteins by glucose. *Biochem J*. 1999; 344:109–116. [PubMed: 10548540]
5. Mossine VV, Mawhinney TP. 1-Amino-1-deoxy-D-fructose (“fructosamine”) and its derivatives. *Adv Carbohydr Chem Biochem*. 2010; 64:291–402. [PubMed: 20837201]
6. Mester L, Mester M, Bhargava KP, Labrid C, Dureng G, Cheucle M. Sugar derivatives of indolamines. Part V: cardiovascular effects and anti-stress activity of desoxyfructose derivative of serotonin and 5-methoxy-tryptamine. *Thrombosis Research*. 1979; 15:245–254. [PubMed: 290049]
7. Dyer DG, Dunn JA, Thorpe SR, Bailie KE, Lyons TJ, McCance DR, Baynes JW. Accumulation of Maillard reaction products in skin collagen in diabetes and aging. *J Clin Invest*. 1993; 91:2463–2469. [PubMed: 8514858]
8. Miyazawa T, Nakagawa K, Shimasaki S, Nagai R. Lipid glycation and protein glycation in diabetes and atherosclerosis. *Amino Acids (Vienna)*. 2012; 42:1163–1170.
9. Narayanan TK, Said S, Mukherjee J, Christian B, Satter M, Dunigan K, Shi B, Jacobs M, Bernstein T, Padma M, Mantil J. Comparative study on the uptake and incorporation of radiolabeled fluorodeoxyglucose, methionine and choline in human astrocytoma. *Mol Imag Biol*. 2002; 4:147–156.
10. Schmidt KC, Lucignani G, Sokoloff L. Fluorine-18-fluorodeoxyglucose PET to determine regional cerebral glucose utilization: a re-examination. *J Nucl Med*. 1996; 37:394–399. [PubMed: 8667082]
11. Thygesen MB, Munch H, Sauer J, Clo E, Jorgensen MR, Hindsgaul O, Jensen KJ. Nucleophilic catalysis of carbohydrate oxime formation by anilines. *J Org Chem*. 2009; 75:1752–1755.
12. Kolb HC, Finn MG, Sharpless B. Click chemistry: diverse chemical function from a few good reactions. *Angew Chem Int Ed*. 2001; 40:2004–2021.
13. Bejot R, Carrol L, Bhakoo K, Declerck J, Gouverneur V. A fluorous and click approach for screening potential PET probes: evaluation of potential hypoxia biomarkers. *Bioorg Med Chem*. 2012; 20:324–329. [PubMed: 22130421]
14. Patel H, Patel B, Pan M, Liang C, Mukherjee M, Mukherjee J. Norepinephrine effects on A $\beta$ -amyloid plaques in post-mortem Alzheimer's disease brain. *J Nucl Med*. 2013; 54(S2):1790.

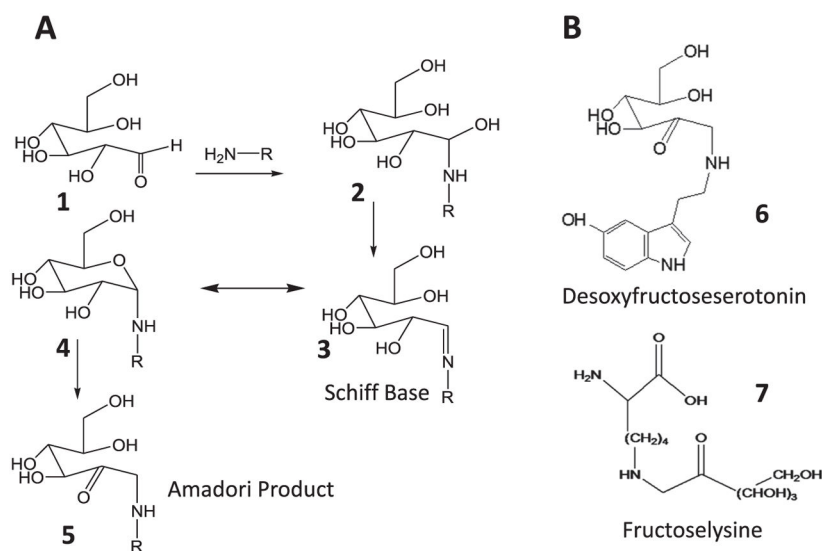
15. Tessier FJ. The Maillard reaction in the human body. The main discoveries and factors that affect glycation. *Pathol Biol.* 2010; 58:214–219. [PubMed: 19896783]

Author Manuscript

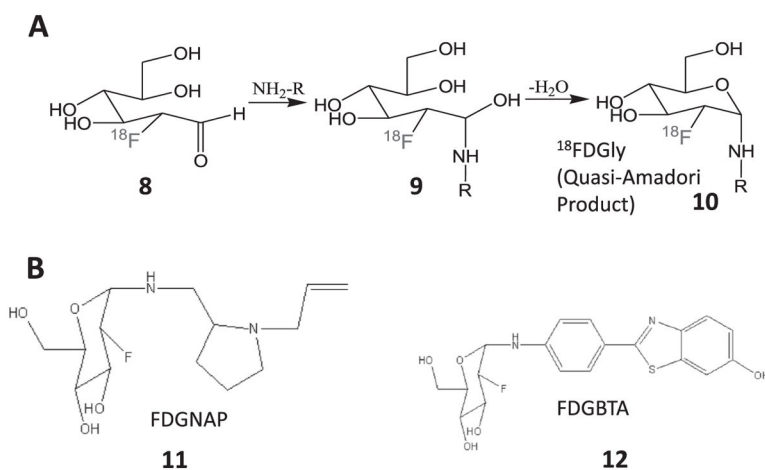
Author Manuscript

Author Manuscript

Author Manuscript



**Figure 1.** (A) Reaction scheme showing Maillard reaction of glucose (**1**) and substituted amine resulting in the formation of Schiff base (**3**) and subsequent isomerization to the Amadori product (**5**). (B) Example of Amadori products, desoxyfructoseserotonin (**6**), and fructoselysine (**7**).

**Figure 2.**

(A) Generic synthesis scheme of  $^{18}\text{F}$ -FDG (**8**) with amines leading to the  $^{18}\text{F}$ -FDGly (**10**), quasi-Amadori product. This is expected from reaction of  $^{18}\text{F}$ -FDG with amines. (B) Two synthesized FDGly products are reported here: FDGNAP (**11**) and FDGBTA (**12**).

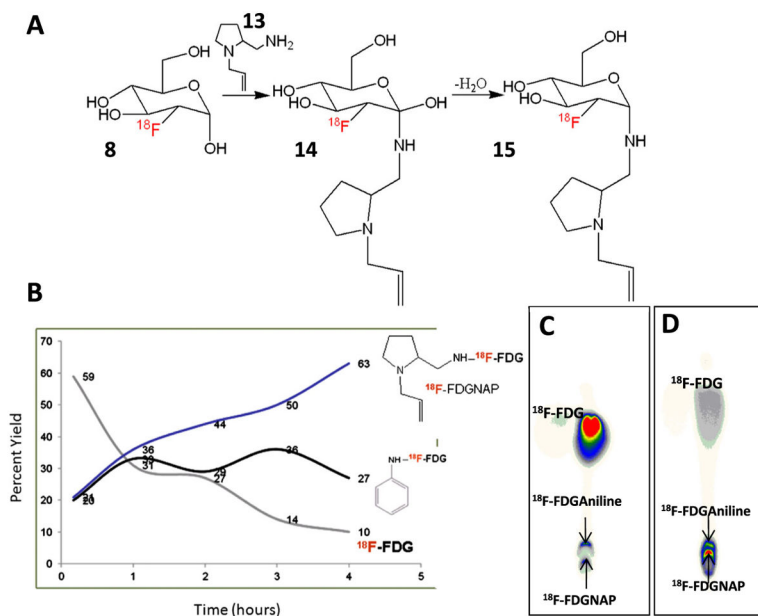


**Figure 3.** (A) Radiosynthesis of  $^{18}\text{F}$ -FDGNAP (**15**) showing reaction of  $^{18}\text{F}$ -FDG (**8**) with NAP (**13**) and subsequent dehydration of intermediate **14**. (B) Kinetics of  $^{18}\text{F}$ -FDGNAP reaction from 0.17 to 4 h showing progressive increase in radiochemical yield of **15**. (C) Radio-TLC of  $^{18}\text{F}$ -FDGNAP reaction mixture at 10 min of reaction time, showing the presence of product along with some  $^{18}\text{F}$ -FDG, and (D) Radio-TLC at 4h of reaction time showing significant increase in product.

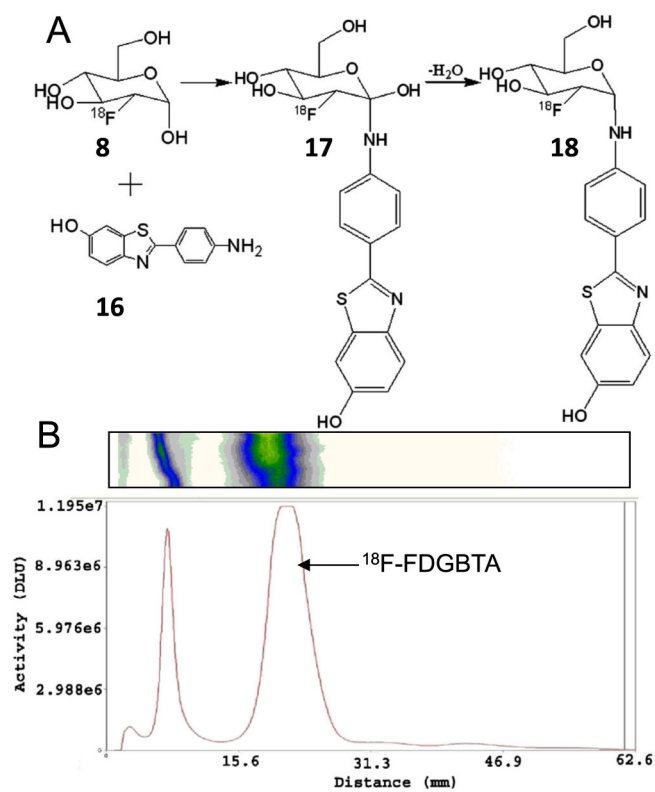


**Figure 4.** (A) Radiosynthesis of  $^{18}\text{F}$ -FDGBTA (**18**) showing reaction of  $^{18}\text{F}$ -FDG (**8**) with BTA (**16**) and subsequent dehydration of intermediate **17**. (B) Radio-TLC of  $^{18}\text{F}$ -FDGBTA (**18**) reaction mixture, showing the presence of product.

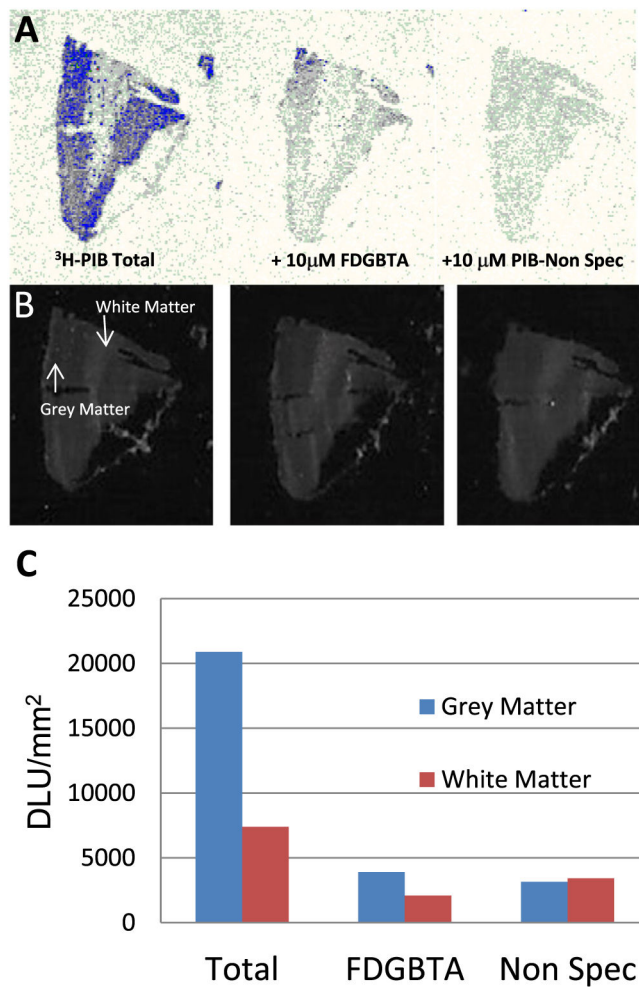


**Figure 5.**

(A) Human postmortem brain autoradiographs showing  $^3\text{H-PIB}$  binding to AD brain slices. Total binding (left), competition with  $10\mu\text{M FDGBTA}$  (middle) and nonspecific binding,  $10\mu\text{M PIB}$  (right). (B) Location of gray matter and white matter on the scanned brain slices of (A). (C) Graph showing the relative displacement of  $^3\text{H-PIB}$  by FDGBTA based on autoradiographs in the gray and white matter.

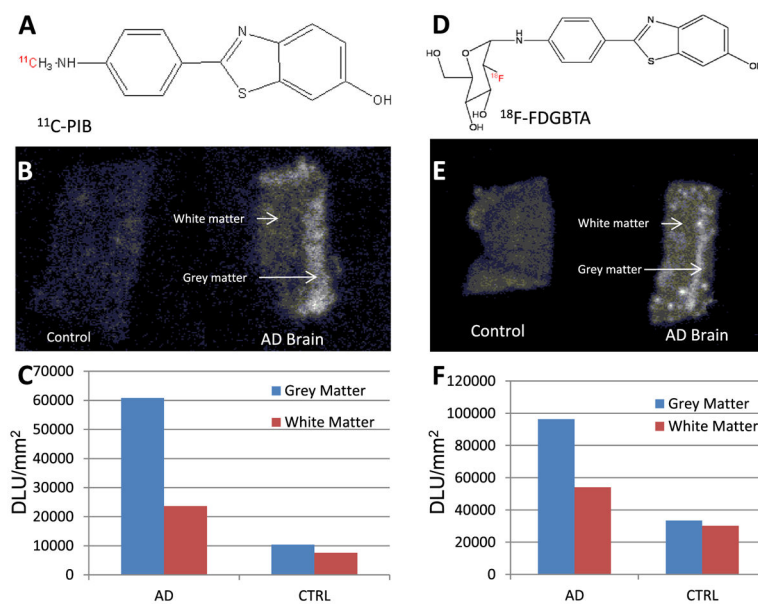


**Figure 6.** (A) Structure of  $^{11}\text{C}$ -PIB. (B) Binding of  $^{11}\text{C}$ -PIB on control versus AD brain. (C) Graph shows the relative binding of  $^{11}\text{C}$ -PIB on control versus AD brain slices based on autoradiographs. (D) Structure of  $^{18}\text{F}$ -FDGBTA. (E) Binding of  $^{18}\text{F}$ -FDGBTA on control versus AD brain. (F) Graph shows the relative binding of  $^{18}\text{F}$ -FDGBTA on control versus AD brain slices based on autoradiographs.